

Palladium(II) induced complete conformational enrichment of the *syn* isomer of *N,N'*-Bis(4-pyridylformyl)piperazine

Debakanta Tripathy, Himansu S. Sahoo, Venkatachalam Ramkumar and Dillip Kumar Chand*

Department of Chemistry, IIT Madras, Chennai, India.

E-mail: dillip@iitm.ac.in; Fax: +914422574202; Tel: +914422574224

Supporting information

Contents:

The file includes ^1H , ^{13}C NMR, H-H COSY, C-H COSY of **L** and **1** (in CDCl_3 and D_2O for **L**; and in D_2O for **1**). ^1H NMR spectrum of **1**' in D_2O . Variable temperature ^1H NMR of **L** in D_2O . Stacking diagram of ^1H NMR of **L** in CDCl_3 , D_2O and DMSO-d_6 . ESI MS for complex **1**', crystallographic information table for **1**' and **L**, ORTEP for **1**' and **L**, energy minimized structures for *syn* and *anti* forms of **L**, complexes **1** and **2**, powder XRD data for pre-crystallized and crystallized **L** and the comparison with simulated spectrum.

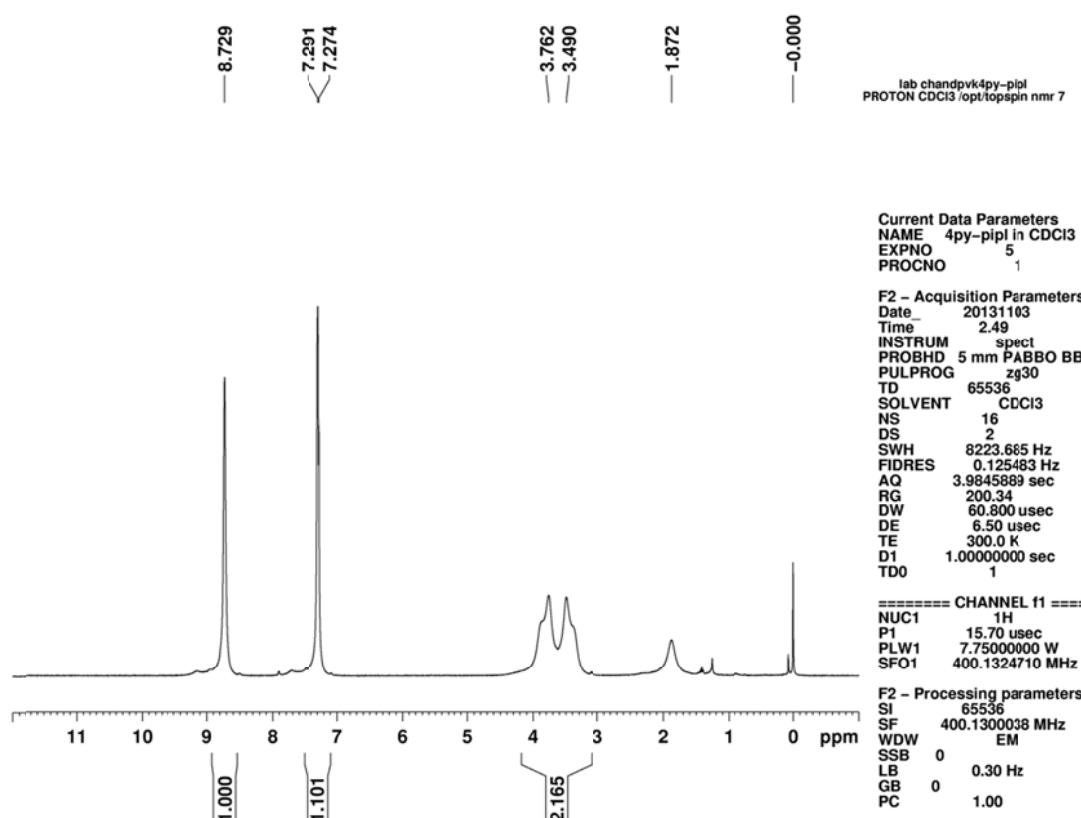


Fig. S1 400 MHz ^1H NMR for **L** in CDCl_3 .

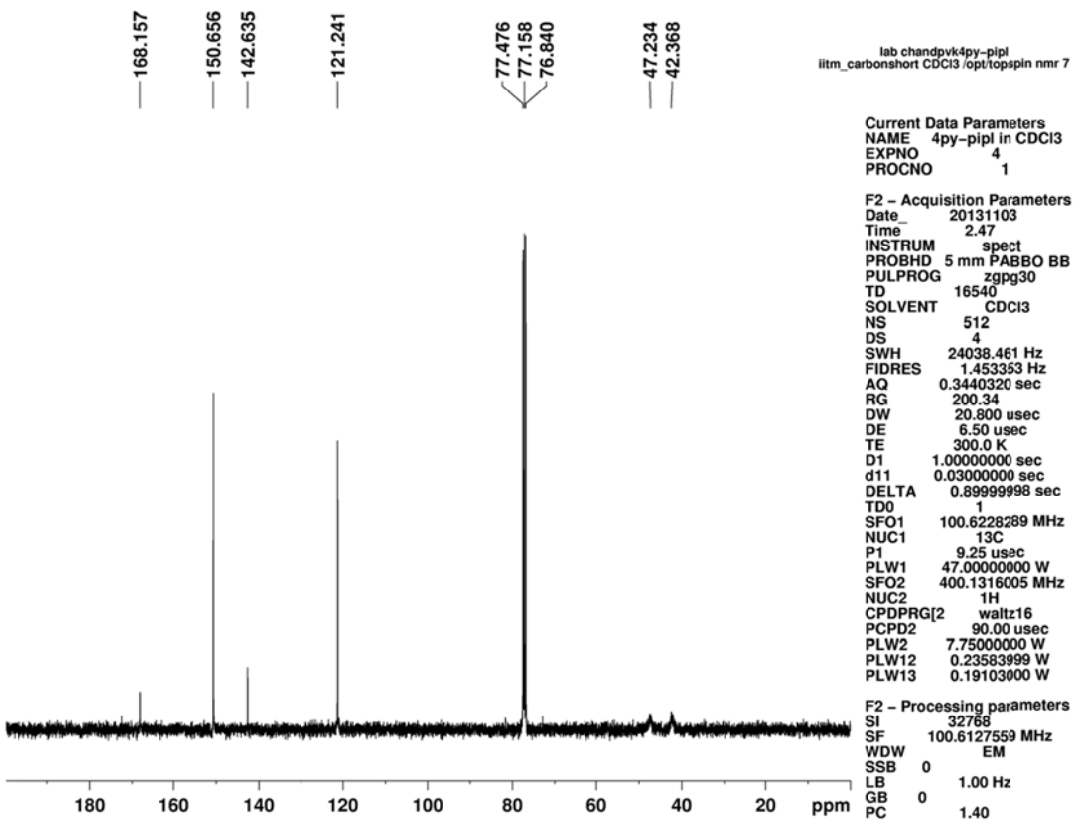


Fig. S2 ¹³C NMR for **L** in CDCl₃.

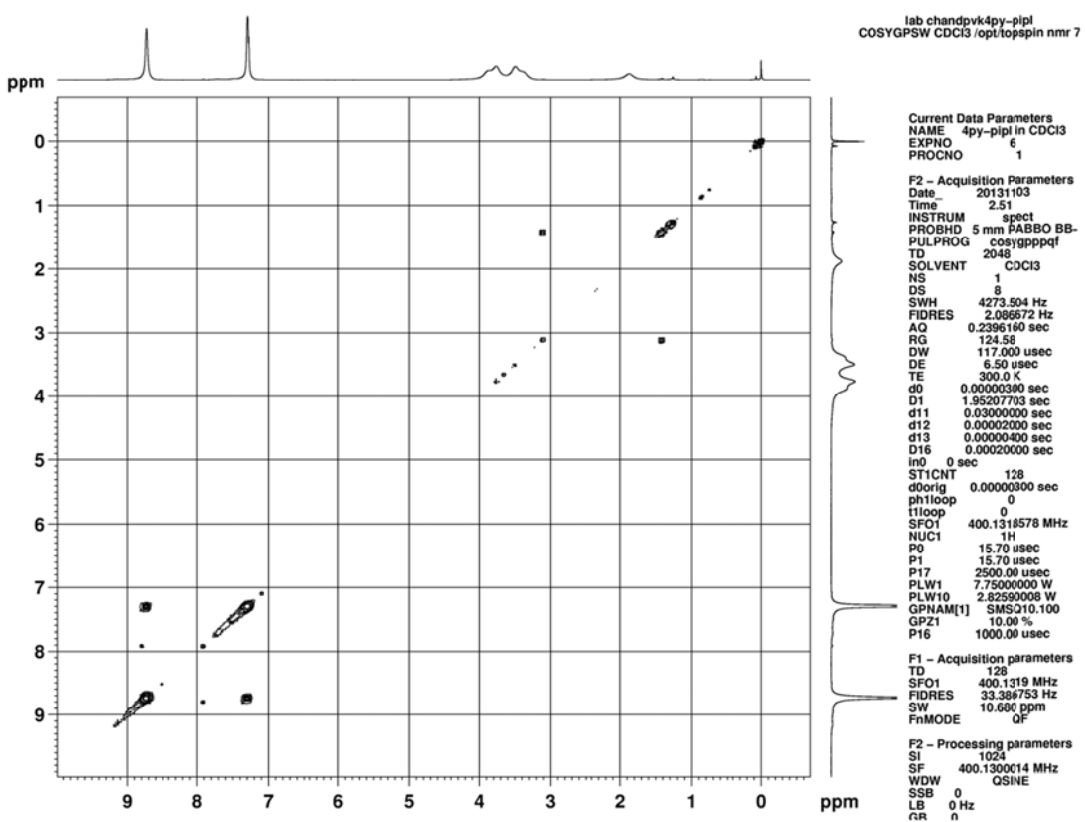


Fig. S3 H-H COSY for **L** in CDCl₃

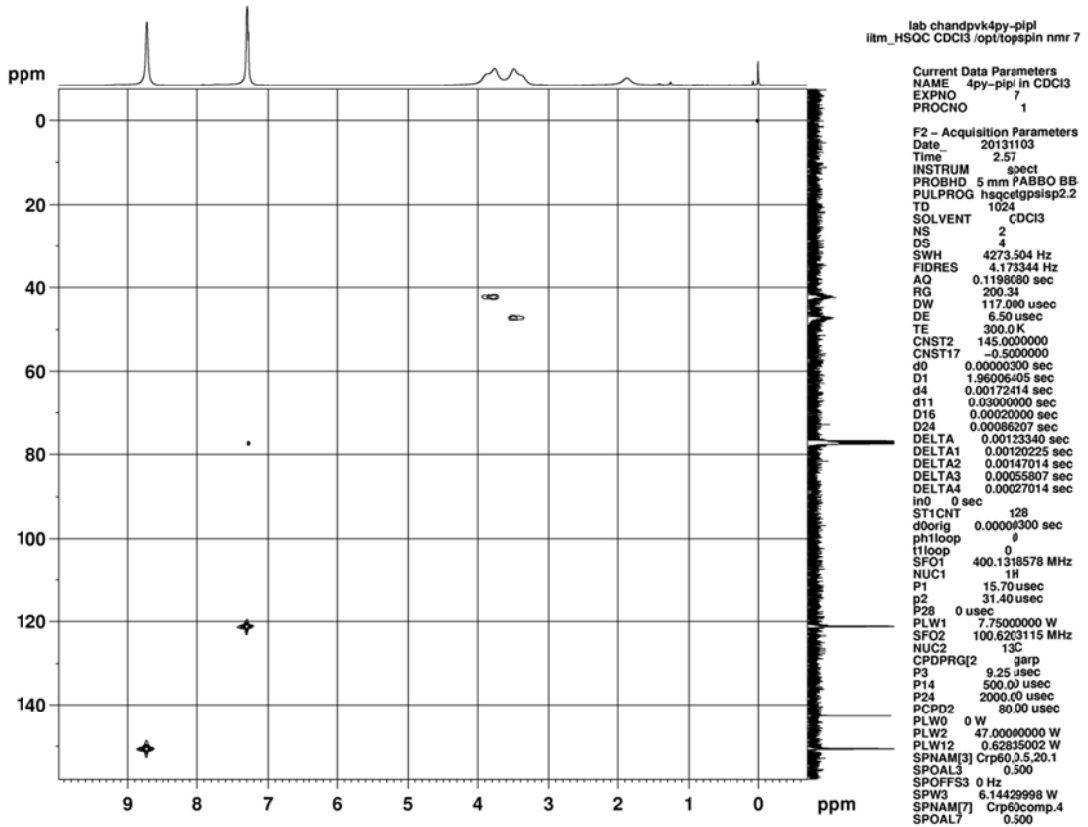


Fig. S4 C-H COSY for L in CDCl₃

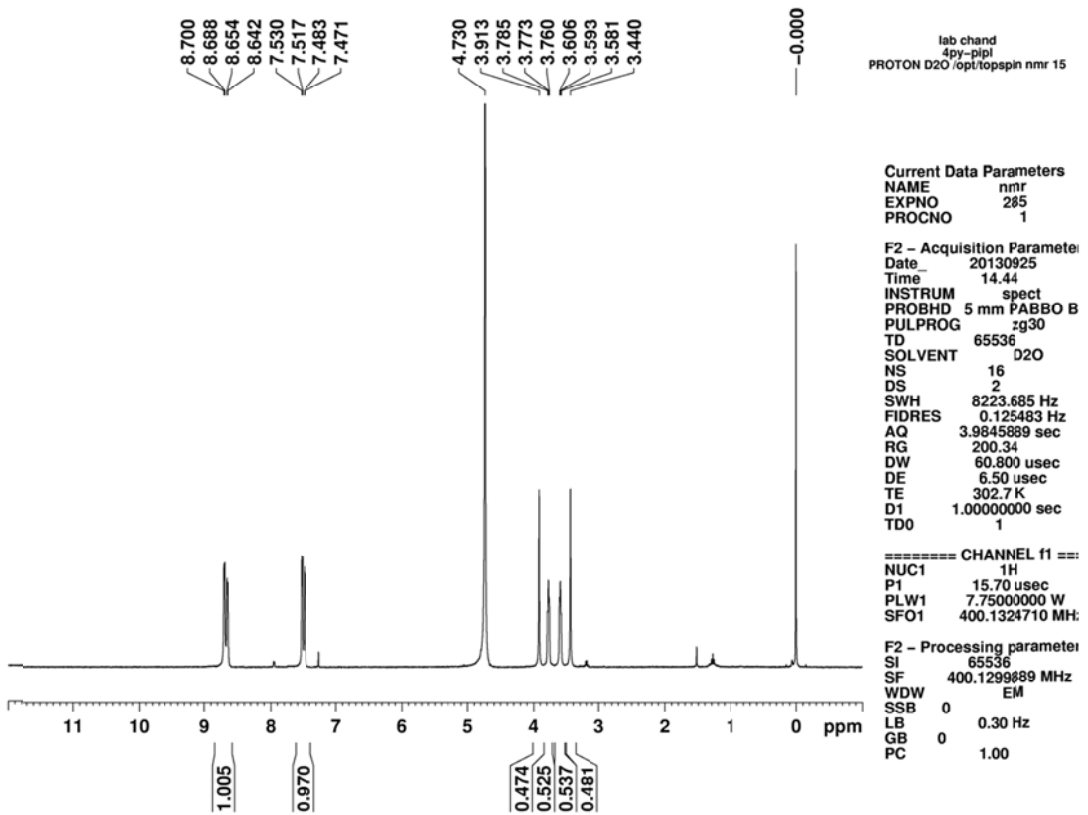


Fig. S5 400 MHz ^1H NMR for **L** in D_2O .

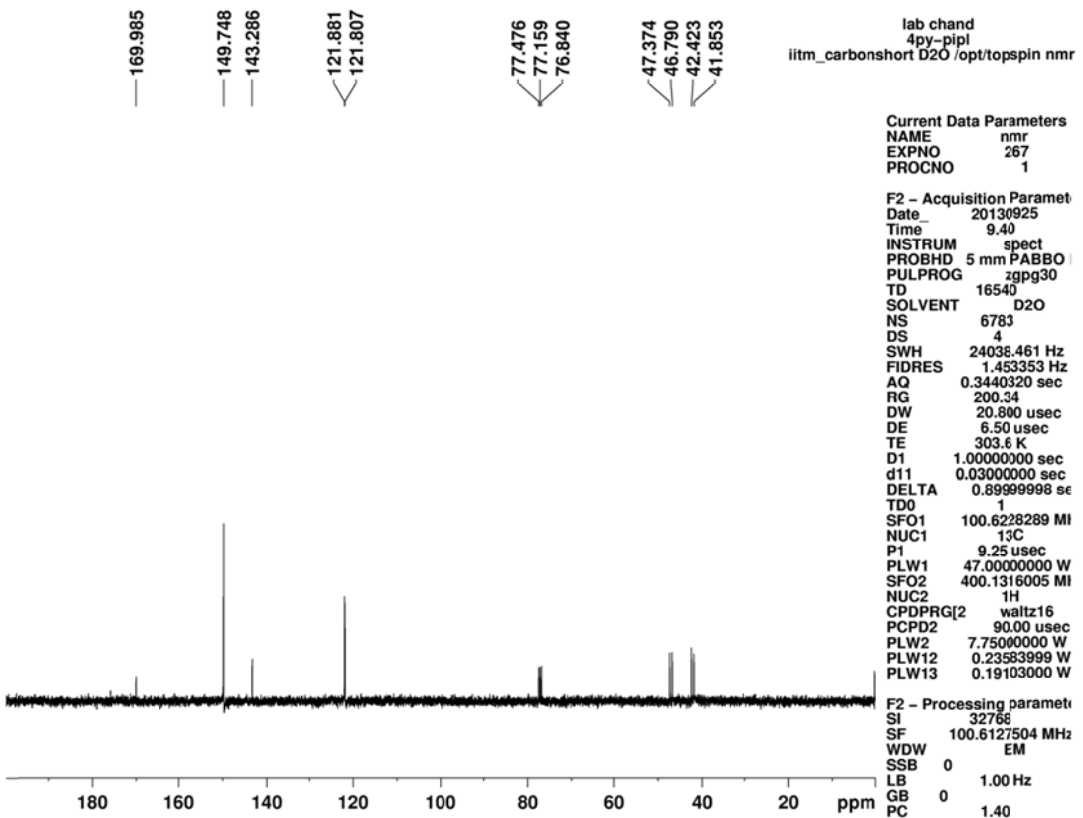


Fig. S6 ¹³C NMR for **L** in D₂O.

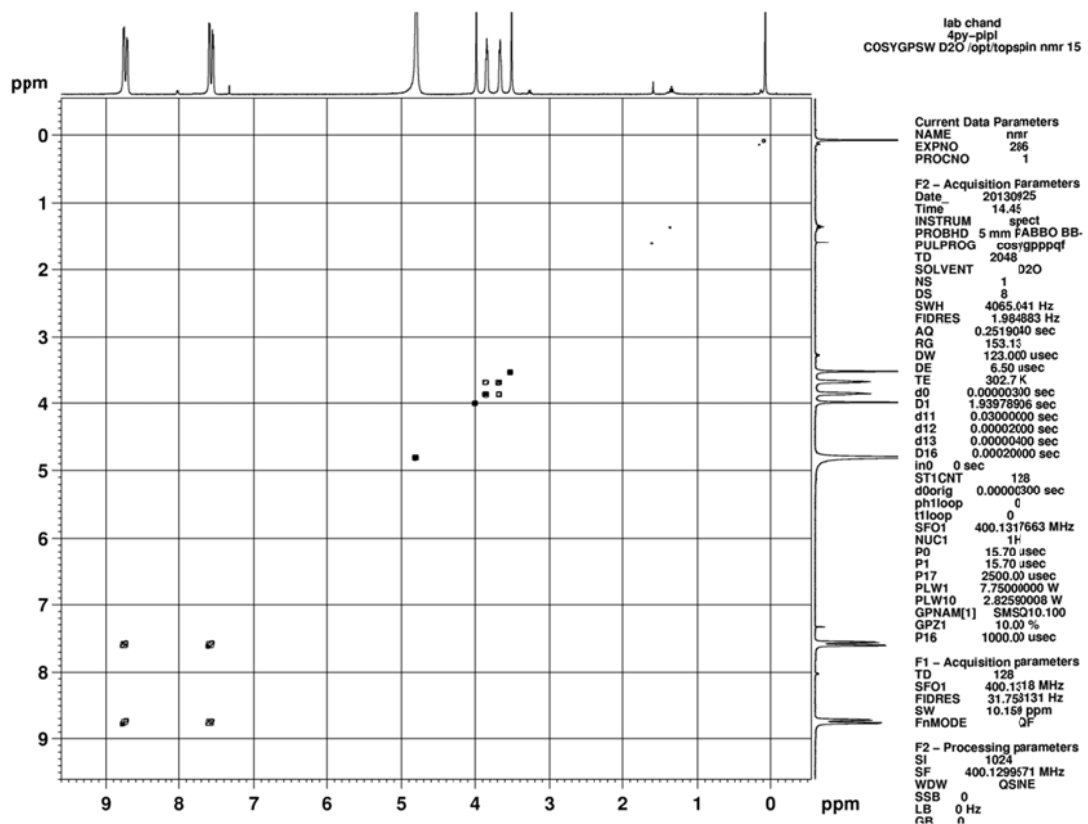


Fig. S7 H-H COSY for **L** in D₂O.

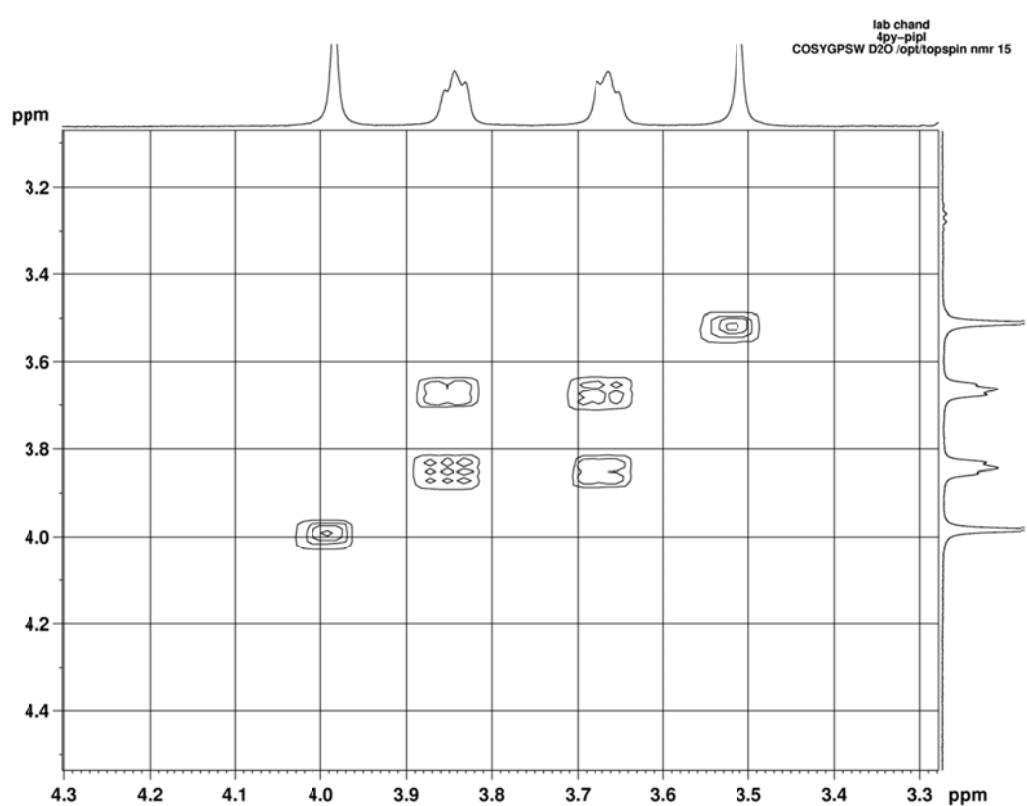


Fig. S8 Expansion of H-H COSY for **L** in D₂O.

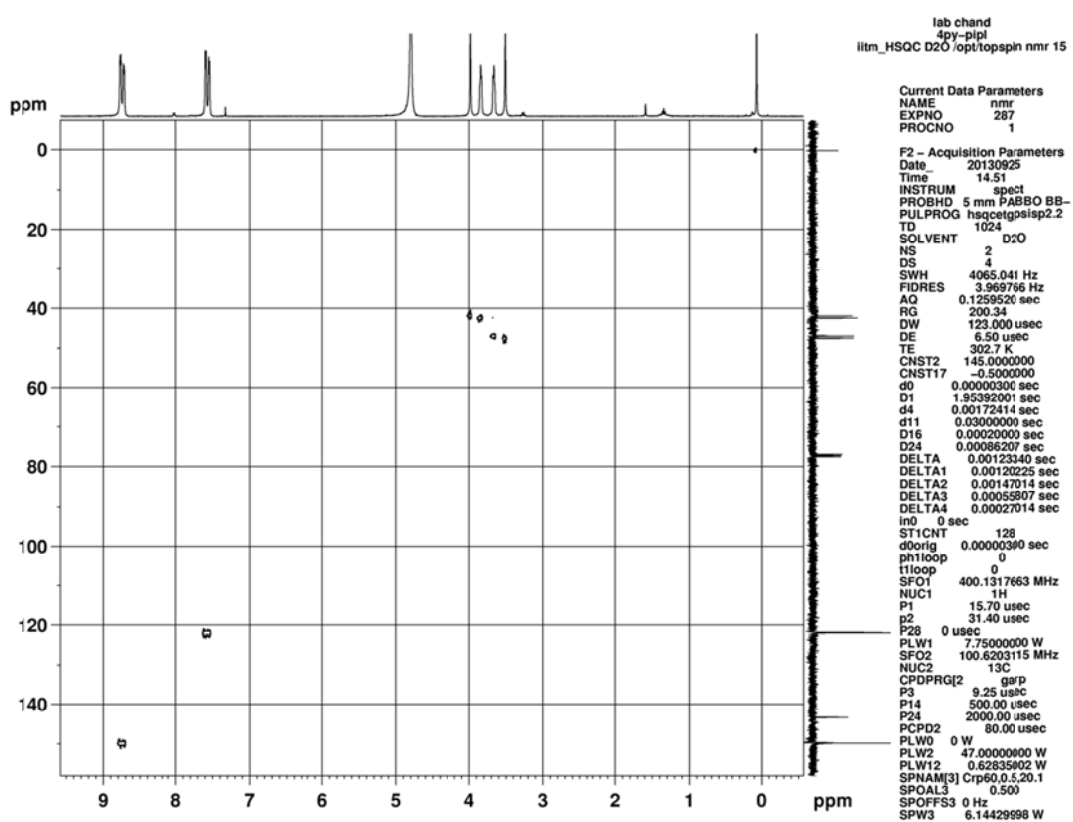


Fig. S9 C-H COSY for **L** in D₂O.

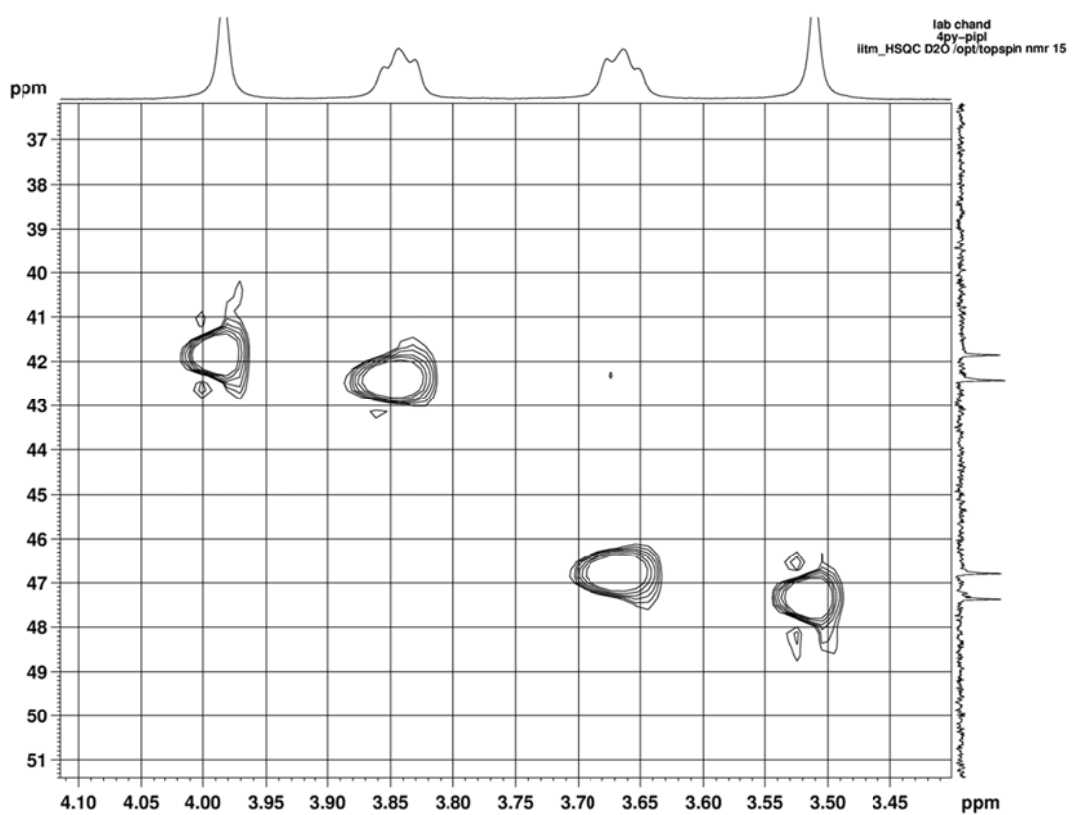


Fig. S10 Expansion of C-H COSY for **L** in D₂O.

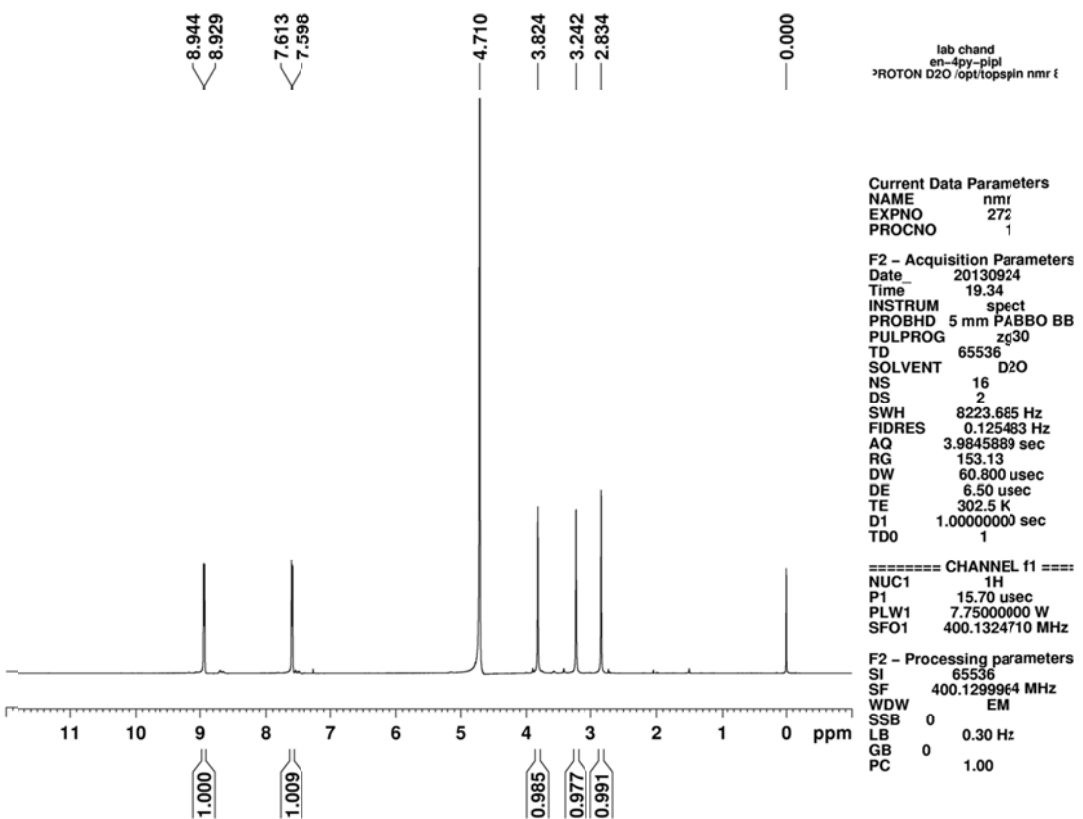


Fig. S11 400 MHz ¹H NMR for **1** in D₂O.

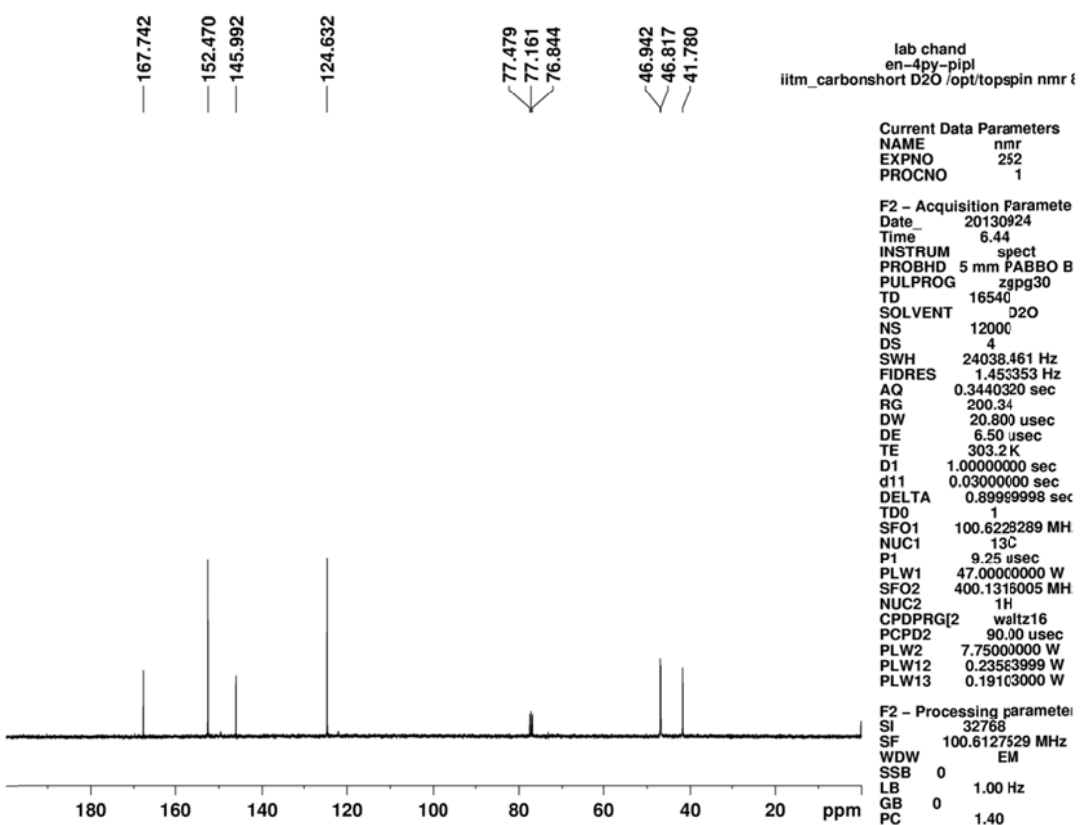


Fig. S12 ^{13}C NMR for **1** in D_2O .

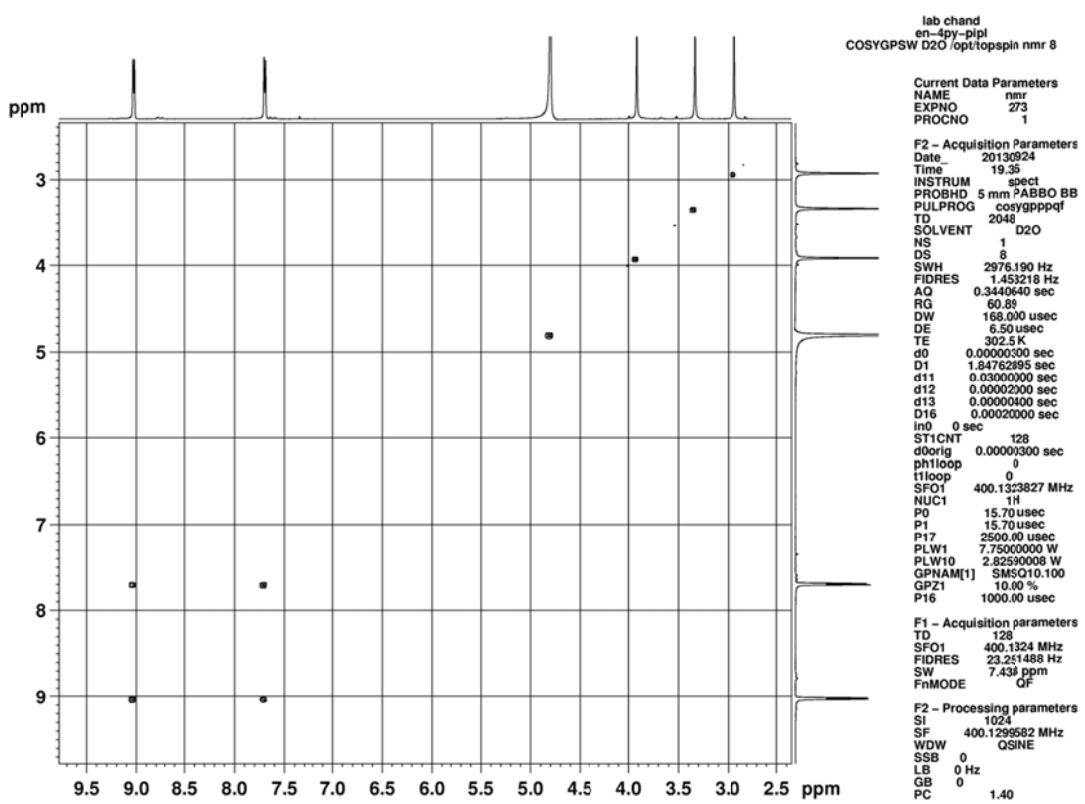


Fig. S13 H-H COSY for **1** in D₂O.

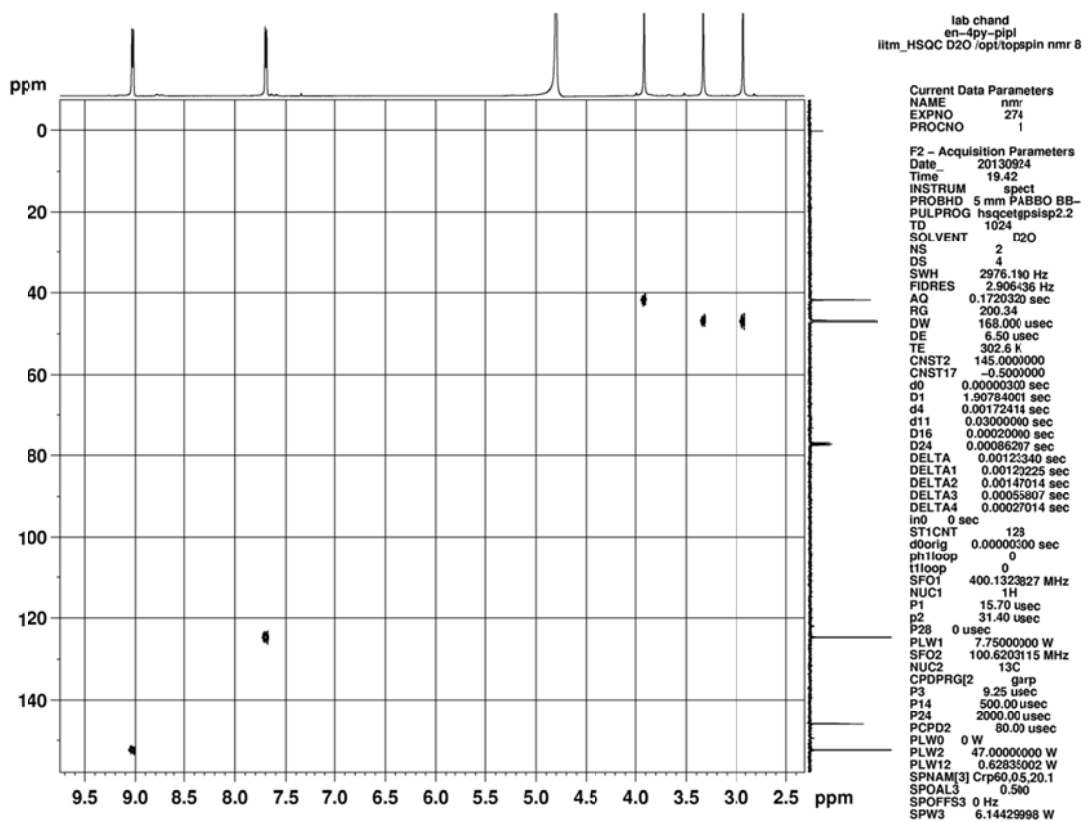


Fig. S14 C-H COSY for **1** in D₂O.

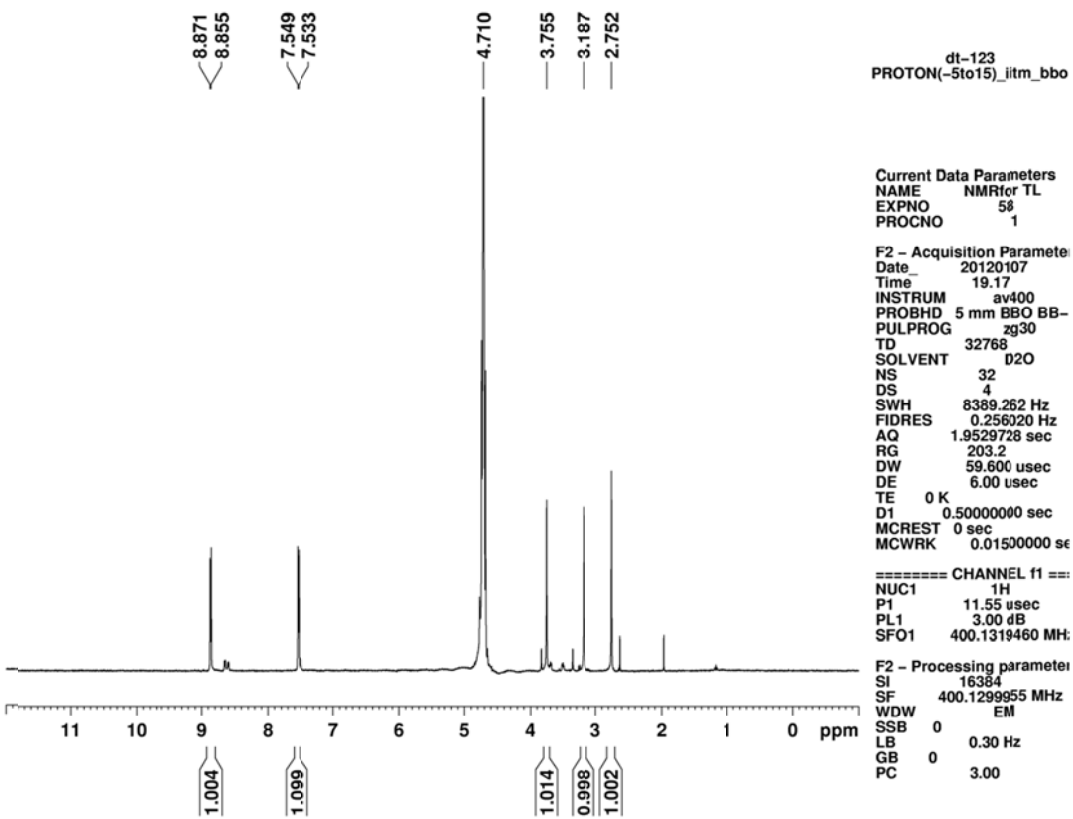


Fig. S15 400 MHz ^1H NMR for **1'** in D_2O .

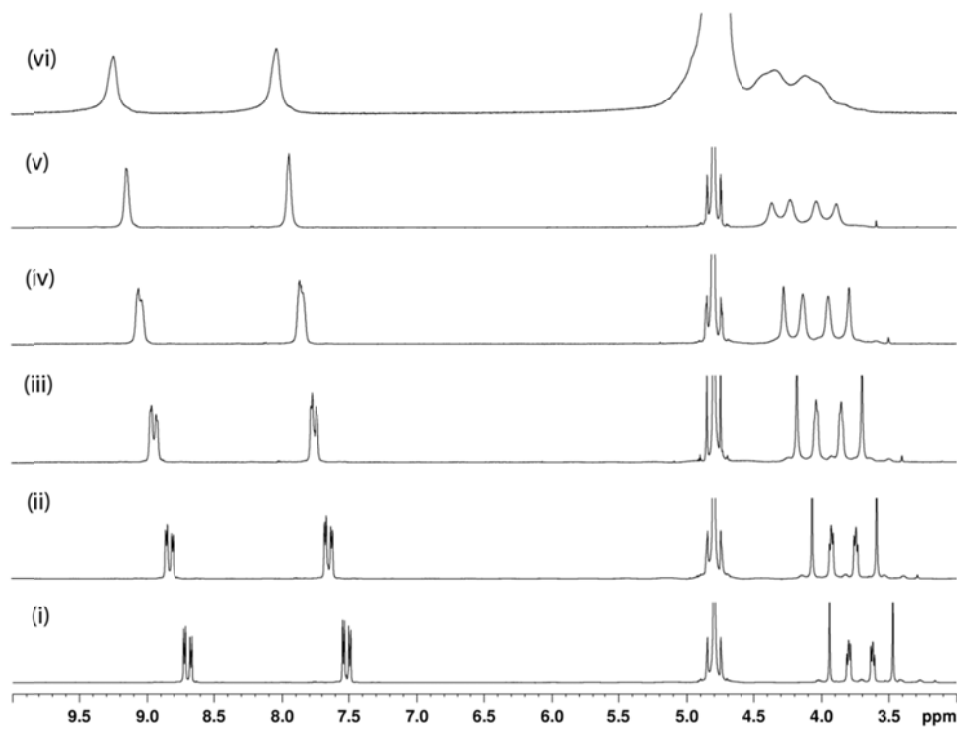


Fig. S16 400 MHz ^1H NMR in D_2O for **L** at different temperatures; (i) 25 °C, (ii) 40 °C, (iii) 50 °C, (iv) 60 °C, (v) 70 °C, and (vi) 80 °C respectively.

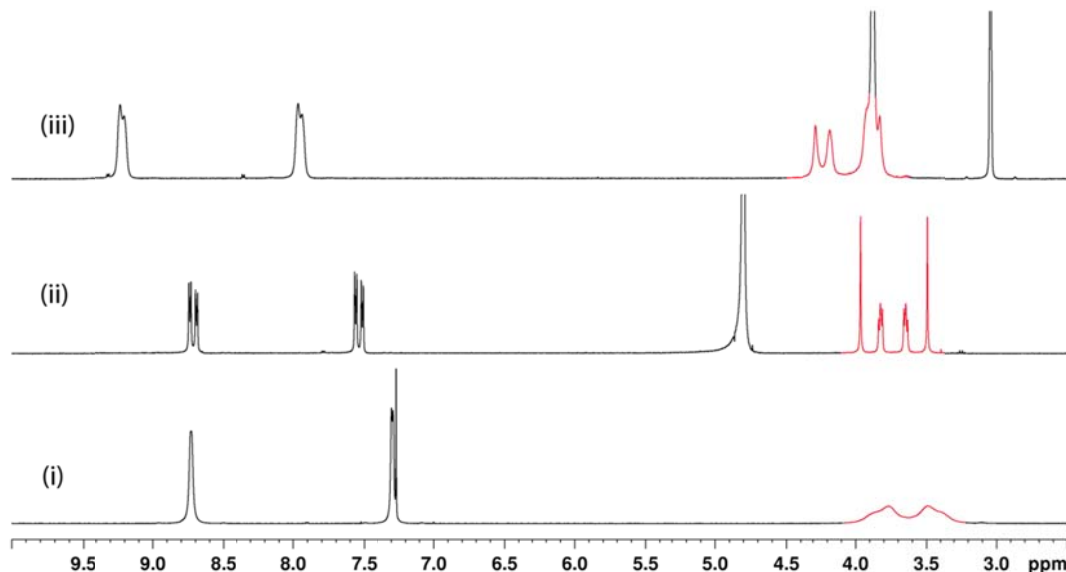


Fig. S17 400 MHz ^1H NMR for **L** recorded in different solvents; in (i) CDCl_3 , (ii) D_2O , and (iii) DMSO-d_6 . The signals shown in red color belongs to the piperazine protons.

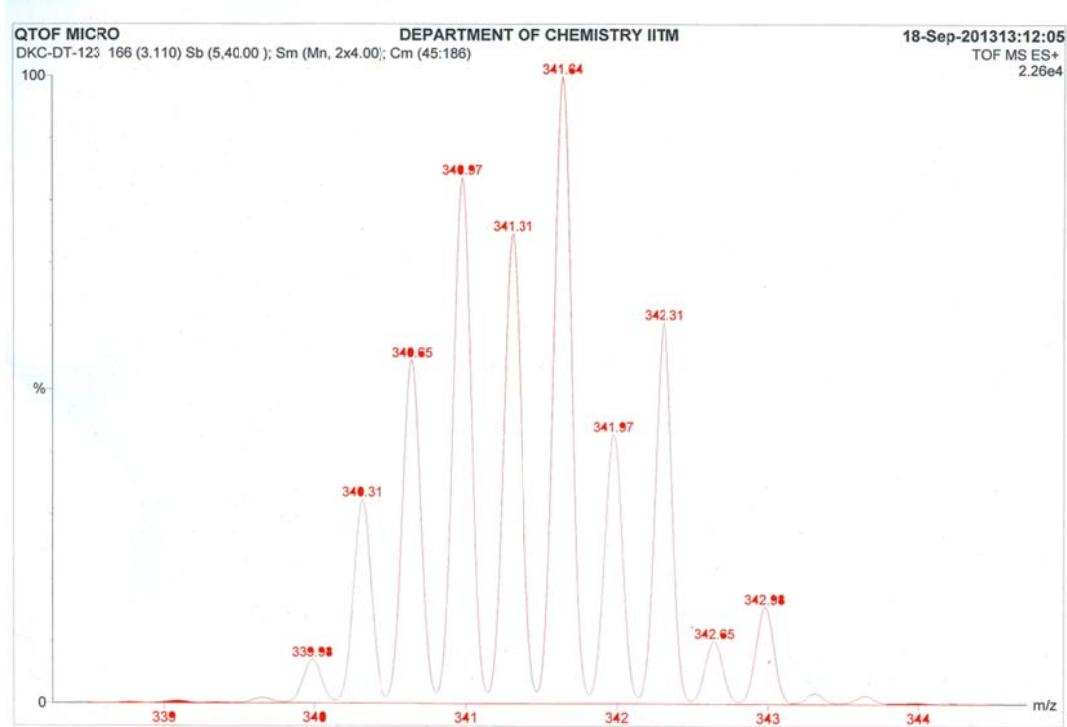


Fig. S18 ESI MS spectrum for complex **1'** showing isotopic distribution pattern for the peak at $m/z = 341$ corresponding to $[1'-3\text{ClO}_4]^{3+}$.

Table S1 Summary of X-ray crystallographic data collection and refinement parameters for **1'**

Empirical formula	C36 H48 Cl4 N12 O23 Pd2
Formula weight	1371.46
Temperature (<i>T</i>)	293(2) K
Wavelength (λ)	0.71073 Å
Crystal system, space group	Orthorhombic, Cmc2(1)
Unit cell dimensions	
<i>a</i> = 18.8926(6) Å	
<i>b</i> = 17.6085(6) Å	
<i>c</i> = 17.0599(6) Å	
Volume (<i>V</i>)	5675.3(3) Å ³
Z, Calculated density	4, 1.605 mg/m ³
Absorption coefficient	0.906 mm ⁻¹
F(000)	2768
Crystal size	0.35 x 0.28 x 0.26 mm
Theta range for data collection	1.58 to 25.00°.
Reflections collected/unique	32532 / 5142 [R(int) = 0.0262]
Completeness to theta = 25.00	100.0 %
Absorption correction	None
Max. and min. transmission	0.7985 and 0.7421
Refinement method	Full-matrix least-squares on F ²
Data / restraints / parameters	5142 / 5 / 369
Goodness-of-fit on F ²	1.122
Final R indices [I>2sigma(I)]	<i>RI</i> = 0.0405, <i>wR2</i> = 0.1244
R indices (all data)	<i>RI</i> = 0.0465, <i>wR2</i> = 0.1341
Largest diff. peak and hole	0.821 and -0.444 e.Å ⁻³

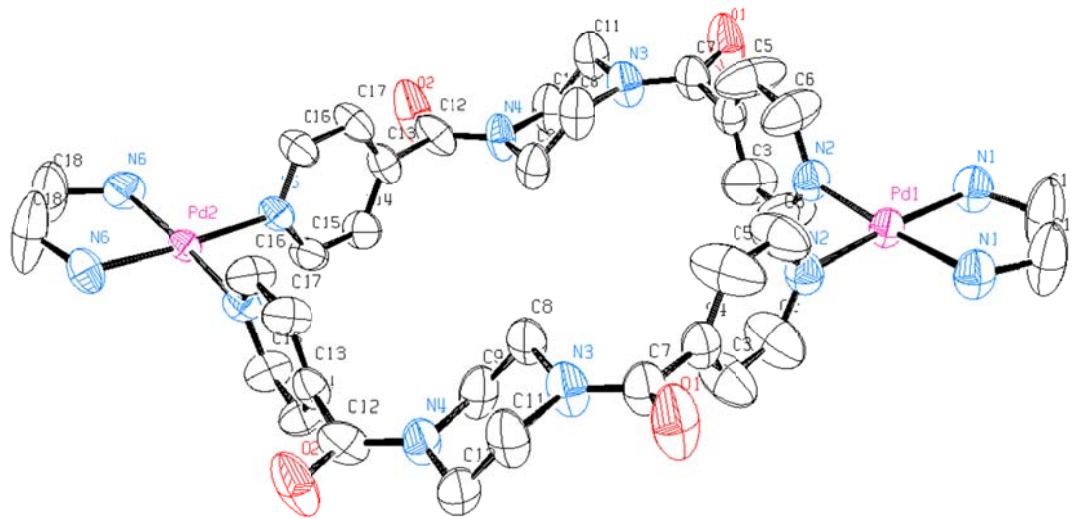


Fig. S19 ORTEP diagram for complex **1'**. Hydrogen atoms, solvent molecules and anions are excluded for clarity. Thermal ellipsoids are shown in 50% probability level.

Table S2: Summary of X-ray crystallographic data collection and refinement parameters for **L**

Empirical formula C16H16N4O2

Formula weight 296.33

Temperature 298(2) K

Wavelength 0.71073 Å

Crystal system, space group Monoclinic, P2(1)/n

Unit cell dimensions

a = 9.1945(6) Å

b = 8.2633(5) Å

c = 9.9539(6) Å

 β = 107.528(2) $^\circ$.Volume (V) 721.15(8) Å³Z, Calculated density 4, 1.387 mg/m³Absorption coefficient 0.125 mm⁻¹

F(000) 308

Crystal size 0.25 x 0.20 x 0.15 mm

Theta range for data collection 2.65 to 25.00 deg.

Reflections collected / unique 4185 / 1211 [R_{int}] = 0.0213]

Completeness to theta = 25.00 95.7 %

Absorption correction Multi-scan

Max. and min. transmission 0.9815 and 0.9695

Refinement method Full-matrix least-squares on F²

Data / restraints / parameters 1211 / 0 / 101

Goodness-of-fit on F² 1.068Final R indices [I>2sigma(I)] R_I = 0.0367, wR_2 = 0.1259R indices (all data) R_I = 0.0466, wR_2 = 0.1378

Extinction coefficient 0.094(16)

Largest diff. peak and hole 0.184 and -0.148 e.Å⁻³

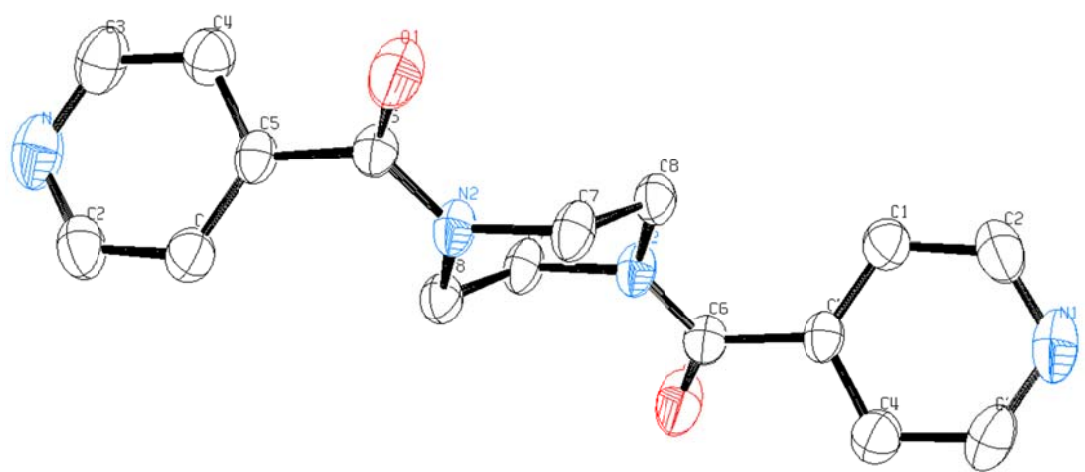


Fig. S20 ORTEP diagram for **L**. Hydrogen atoms are excluded for clarity. Thermal ellipsoids are shown in 50% probability level.

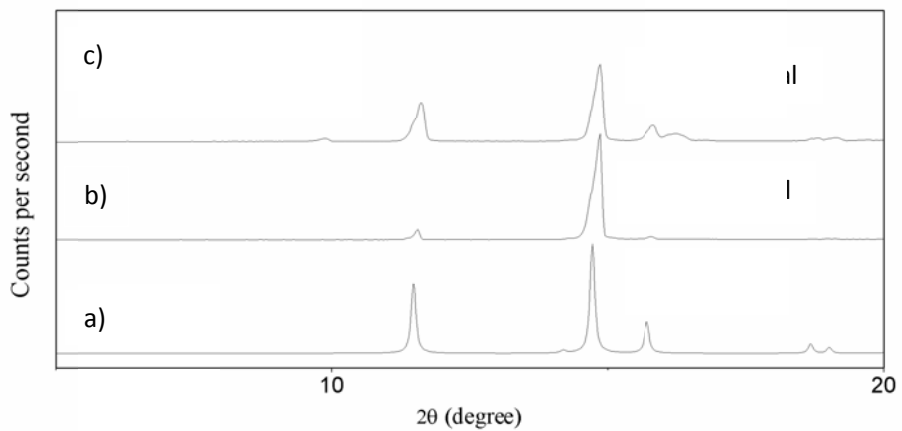


Fig. S21 Powder-XRD data for the ligand **L**; a) simulated from the single crystal X-ray data, (b-c) experimental diffraction pattern for **L** b) after re-crystallization from water and c) after re-crystallization from DCM

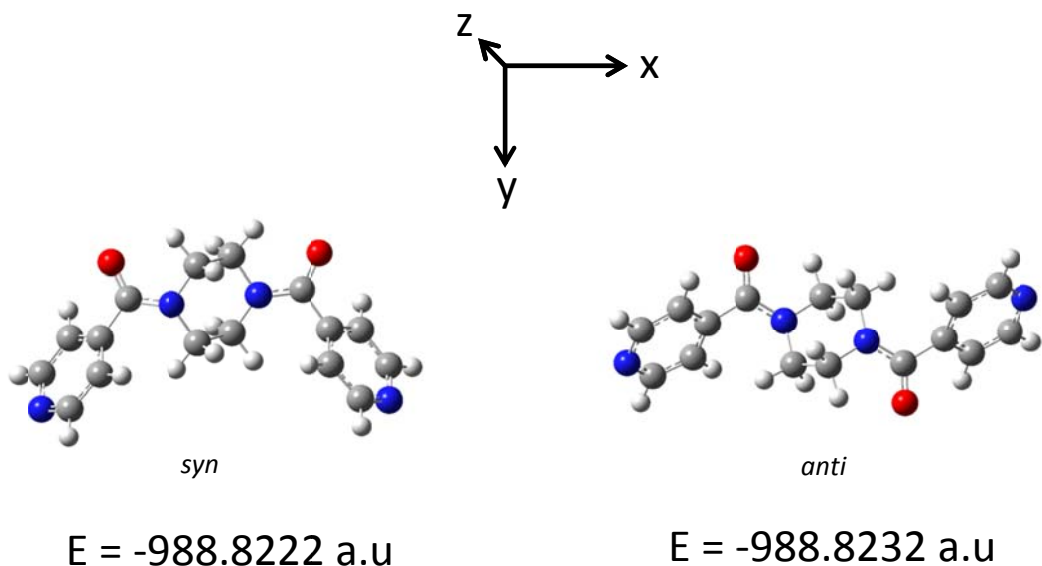
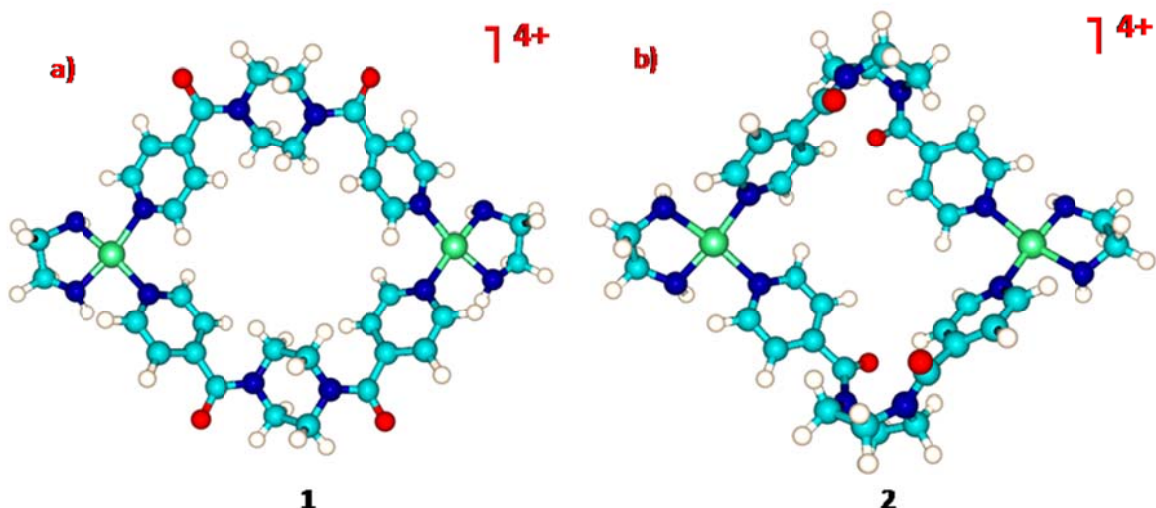


Fig. S22 Energy minimized structure for both *syn* and *anti*-conformations obtained by DFT calculations.



$$H_{corr} = E_{tot} - k_{BT} = \mathbf{535.18 \text{ kcal mole}^{-1}}$$

$$G_{corr} = H_{corr} - TS_{corr} = \mathbf{441.32 \text{ kcal mole}^{-1}}$$

$$\varepsilon_0 + H_{corr} = \mathbf{-1636118.22 \text{ kcal mol}^{-1}}$$

$$\varepsilon_0 + G_{corr} = \mathbf{-1636212.08 \text{ kcal mol}^{-1}}$$

$$H_{corr} = E_{tot} - k_{BT} = \mathbf{536.41 \text{ kcal mole}^{-1}}$$

$$G_{corr} = H_{corr} - TS_{corr} = \mathbf{444.74 \text{ kcal mole}^{-1}}$$

$$\varepsilon_0 + H_{corr} = \mathbf{-1636114.94 \text{ kcal mol}^{-1}}$$

$$\varepsilon_0 + G_{corr} = \mathbf{-1636206.61 \text{ kcal mol}^{-1}}$$

Fig. S23 Energy minimized structure for complexes of Pd(II) with **L**; a) in *syn*-conformation and b) in *anti*-conformation obtained by DFT calculations using B3LYP-LANL2DZ basis sets as included in *Gaussian 09* package¹ (corresponding thermodynamic parameters are listed below the structures).

Reference

1. M. J. Frisch, G. W. Trucks, H. B. Schlegel, G. E. Scuseria, M. A. Robb, J. R. Cheeseman, G. Scalmani, V. Barone, B. Mennucci, G. A. Petersson, H. Nakatsuji, M. Caricato, X. Li, H. P. Hratchian, A. F. Izmaylov, J. Bloino, G. Zheng, J. L. Sonnenberg, M. Hada, M. Ehara, K. Toyota, R. Fukuda, J. Hasegawa, M. Ishida, T. Nakajima, Y. Honda, O. Kitao, H. Nakai, T. Vreven, J. A. Montgomery, Jr., J. E. Peralta, F. Ogliaro, M. Bearpark, J. J. Heyd, E. Brothers, K. N. Kudin, V. N. Staroverov, T. Keith, R. Kobayashi, J. Normand, K. Raghavachari, A. Rendell, J. C. Burant, S. S. Iyengar, J. Tomasi, M. Cossi, N. Rega, J. M. Millam, M. Klene, J. E. Knox, J. B. Cross, V. Bakken, C. Adamo, J. Jaramillo, R. Gomperts, R. E. Stratmann, O. Yazyev, A. J. Austin, R. Cammi, C. Pomelli, J. W. Ochterski, R. L. Martin, K. Morokuma, V. G. Zakrzewski, G. A. Voth, P. Salvador, J. J. Dannenberg, S. Dapprich, A. D. Daniels, O. Farkas, J. B. Foresman, J. V. Ortiz, J. Cioslowski and D. J. Fox, GAUSSIAN 09 (Revision C.01), Gaussian Inc., Wallingford CT, 2010.